


## Article

# The Source and Significance of Silicon in the Late Permian Dalong Formation, Northeastern Sichuan Basin

Xiaotong Ge <sup>1,2,3,\*</sup>, Xun Ge <sup>1,2,3</sup>, Daizhao Chen <sup>4</sup>, Yali Liu <sup>1,2,3</sup>, Ruyue Wang <sup>1,2,3</sup>  and Min Li <sup>1,2,3</sup>

<sup>1</sup> State Key Laboratory of Shale Oil and Gas Enrichment Mechanisms and Efficient Development, Beijing 102206, China; wangruiyue.syky@sinopec.com (R.W.)

<sup>2</sup> Sinopec Key Laboratory of Shale Oil/Gas Exploration and Production Technology, Beijing 102206, China

<sup>3</sup> Petroleum Exploration and Production Research Institute, SINOPEC, Beijing 102206, China

<sup>4</sup> Key Laboratory of Cenozoic Geology and Environment, Institute of Geology and Geophysics, Chinese Academy of Sciences, Beijing 100029, China

\* Correspondence: gexiaotong.syky@sinopec.com

**Abstract:** The Late Permian was a critical interval in geological history, during which dramatic changes occurred in the Earth's surface system, and a set of black rock series rich in organic matter and silicon, the Dalong Formation, was deposited in the northeastern Sichuan Basin. We conducted a detailed sedimentological and petrological investigation integrated with (major and trace) element contents in the deep-water sequence of the Xibeixiang and Jianfeng sections. It demonstrates the source of silicon, tectonic background, and sedimentary environment of the Dalong Formation, and explores the influence of hydrothermal activities on organic matter enrichment. The results show that the upper part of the Dalong Formation contained more radiolarians in the Xibeixiang section compared to the Jianfeng section. Hydrothermal proxies such as  $Eu/Eu^*$ , Al-Fe-Mn diagram,  $Al/(Al + Fe + Mn)$ , and  $Lu_N/La_N$  suggest a biotic origin for the chert in the Dalong Formation in the Xibeixiang and Jianfeng sections, while the Xibeixiang section was slightly affected by hydrothermal activities. The La-Th-Sc diagram and the La/Sc and Ti/Zr crossplots point to a continental island arc and active continental margin origins for the Xibeixiang and Jianfeng sections. Combined with previous research, the silicon of the Dalong Formation in the northeastern Sichuan Basin is mainly derived from biological sources. The Xibeixiang section was affected by a small amount of hydrothermal fluid due to its proximity to the Paleo-Tethys Ocean and continental island arcs. Furthermore, the enrichment of organic matter was predominantly driven by high productivity, with minimal impact from hydrothermal activities. These insights hold significant research value and practical implications for shale gas exploration in the Sichuan Basin.



Academic Editor: Thomas Gentzis

Received: 23 November 2024

Revised: 10 December 2024

Accepted: 13 December 2024

Published: 13 January 2025

**Citation:** Ge, X.; Ge, X.; Chen, D.; Liu, Y.; Wang, R.; Li, M. The Source and Significance of Silicon in the Late Permian Dalong Formation, Northeastern Sichuan Basin. *Minerals* **2025**, *15*, 69. <https://doi.org/10.3390/min15010069>

**Copyright:** © 2025 by the authors. Licensee MDPI, Basel, Switzerland. This article is an open access article distributed under the terms and conditions of the Creative Commons Attribution (CC BY) license (<https://creativecommons.org/licenses/by/4.0/>).

**Keywords:** northeastern Sichuan Basin; Dalong Formation; source of Silicon; biotic origin; hydrothermal activity

## 1. Introduction

The Upper Permian deep-water succession in the northeast Sichuan Basin is characterized by organic-rich strata, serving as effective source rocks that supply substantial hydrocarbons to nearby gas fields [1]. This depositional succession captures extensive information about the oceanic chemical and physical changes during the Late Permian, providing valuable insights into the silicon source of the Dalong Formation. The formation is stratified from bottom to top with organic-rich marly limestone, shale, siliceous rocks, and siliceous limestone, spread across troughs. The extensive organic-rich siliceous rocks serve

as source materials for shale gas and mineral resources [2]. Understanding the silicon source and sedimentary environment of these rocks is crucial [3], as it governs the formation and accumulation of fossil energy, presenting significant research and economic implications.

Previous studies have reported that the siliceous source of the Dalong Formation in the Yangtze block can be classified into biogenic and hydrothermal origins. In the Lower Yangtze block, the base of the Dalong Formation shows the signature of both origins, with the middle section predominantly biogenic and the top primarily hydrothermal [4]. The bedded chert in the Middle Yangtze block also displays a combination of these origins [5]. However, the silicon source in the Upper Yangtze block remains undetermined. Notably, the Shangsi section and Leba 1 borehole interval are largely characterized by biochemical deposits with some hydrothermal contributions [6,7], while the cherts of the Dalong Formation in the Changjianggou section are believed to have a mixed source of biological origin and volcanic activity [8]. To further elucidate the silicon sources in the northeastern Sichuan region, this study focuses on an organic-rich intrashelf basinal succession of the Upper Permian at the Xibeixiang and Jianfeng sections in Guangyuan, Sichuan Province. Comprehensive analyses including the determination of major and trace elements were conducted. These investigations aimed to clarify the siliceous source, structural background, and sedimentary environment of the organic-rich black rocks within the Dalong Formation. These findings enhance the understanding of the mechanisms behind organic matter enrichment and evaluate the potential of these strata as hydrocarbon source rocks.

## 2. Geological Background

During the Lopingian (Late Permian), the South China Block, comprising the Yangtze and Cathaysia subblocks, was geographically isolated and migrated to the subtropical latitudes (approximately 23–25° N) of the Equatorial Warm Water Province (EWWP), locating at the eastern margin of the Paleo-Tethys Ocean (Figure 1) [9]. In this period, carbonate platforms were prevalent over the Yangtze subblock, especially in the upper Yangtze region, where several intraplateform or intrashelf basins developed (Figure 1). In terms of ancient geography, the Xibeixiang section was situated close to the opening of the Kaijiang–Liangping intraplateform basin, connected to the Qinling Ocean, also known as the Paleo-Tethys. The Jianfeng section was located at the southwestern edge of the Kaijiang–Liangping trough, approximately 35 km northeast of the Shangsi section, with a similar depositional environment and was once considered as an auxiliary candidate for GSSP (Global Stratotype Section and Point) for the P–T boundary [10].

The Xibeixiang section is classified as a deep-water intrashelf facies, where the Dalong Formation, with a total thickness of 36.74 m, rests unconformably on the Wuchiaping Formation (Figure 2a). The formation is distinguished by abundant deep-water fauna, including ammonoids and radiolarians, affirming its relevance to a deep-water intrashelf basinal environment. Stratigraphically, the Dalong Formation is divided into three main parts. The lower part consists of thin-bedded siliceous mudstone and thin- to medium-bedded lime mudstone/wackestone, interspersed with two volcanic ash layers, indicative of the rapid deepening of water depth. The middle part is predominated by organic-rich marly limestone and intercalated with black shales or organic-rich limestones (Figure 2b), reflecting the trend of progressive transgression. The upper part features bedded radiolarian cherts, intercalated with shales and a limestone lens (Figure 2d), transitioning upwards into a limestone succession. This upper limestone succession is characterized by thin- to medium-bedded lime mudstone (Figure 2e) with nektonic ammonite fossils (Figure 2f) and signs of bioturbation, further interspersed with seven layers of volcanic ash (Figure 2g), illustrating complex depositional dynamics.

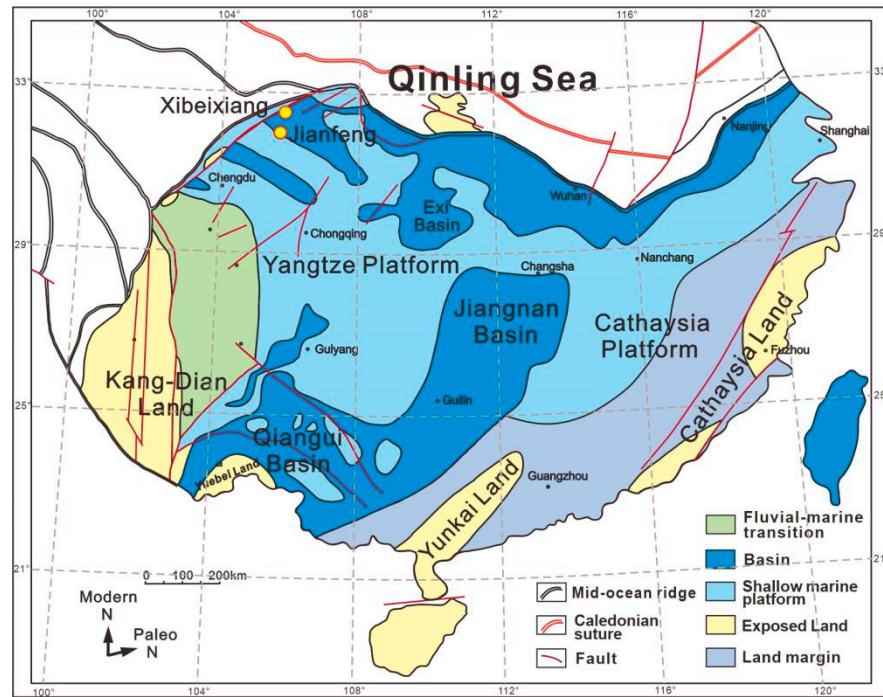


**Figure 1.** Paleogeographic map of South China during the deposition period of the Dalong Formation, showing the location of the Xibeixiang and Jianfeng sections (modified from [11]).

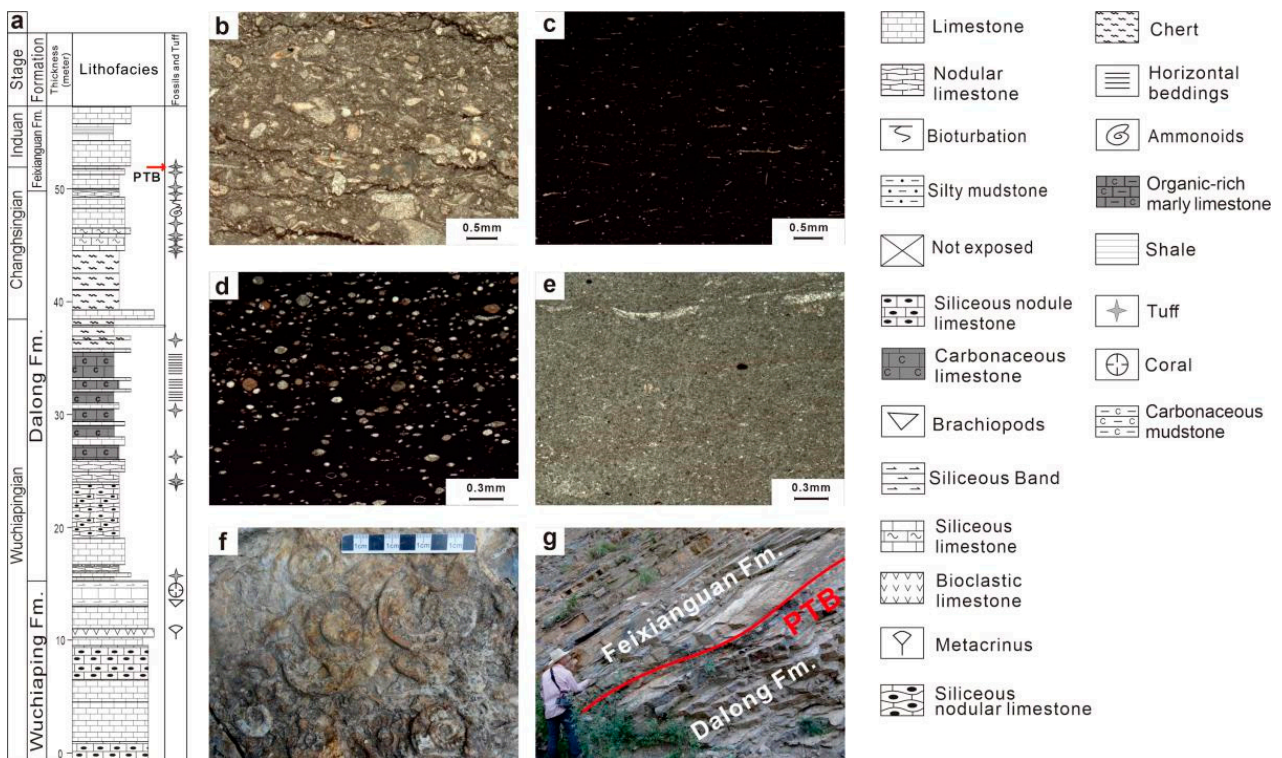


**Figure 2.** (a) The lithological column of the Xibeixiang section. Photomicrographs under plane-polarized light show (b) ampetitic limestone in the middle part of the Dalong Formation, (c) bedded chert bearing large numbers of radiolarians in the upper part of the Dalong Formation, and (e) lime mudstone in the uppermost Dalong Formation. (d) The limestone lens of the upper part of the Dalong Formation. (f) Ammonite fossils in the upper part of the Dalong Formation. (g) The photomicrograph of the Permian-Triassic boundary (PTB). A standing person for scale (1.65 m).

The Jianfeng section exhibits a conformable contact between the Dalong and Wuchiaping formations (Figure 3a). In the lower part of the Dalong Formation, the dominant lithologies are medium-bedded and siliceous limestones. The middle part is characterized by black shale and marly limestone (Figure 3b) interbedded with siliceous rocks and is notable for its abundance of ostracod fossils and an intercalated layer of volcanic ash (Figure 3c), which may have originated from the Emeishan Large Igneous Province [12]. The upper section is characterized by carbonaceous mudstones alternating with radiolarian siliceous rocks (Figure 3d), where the radiolarians are arranged in parallel. This section is capped by two layers of volcanic ash. Above this, the Changhsing Formation is conformably in contact with the Dalong Formation, indicating a continuous depositional sequence.

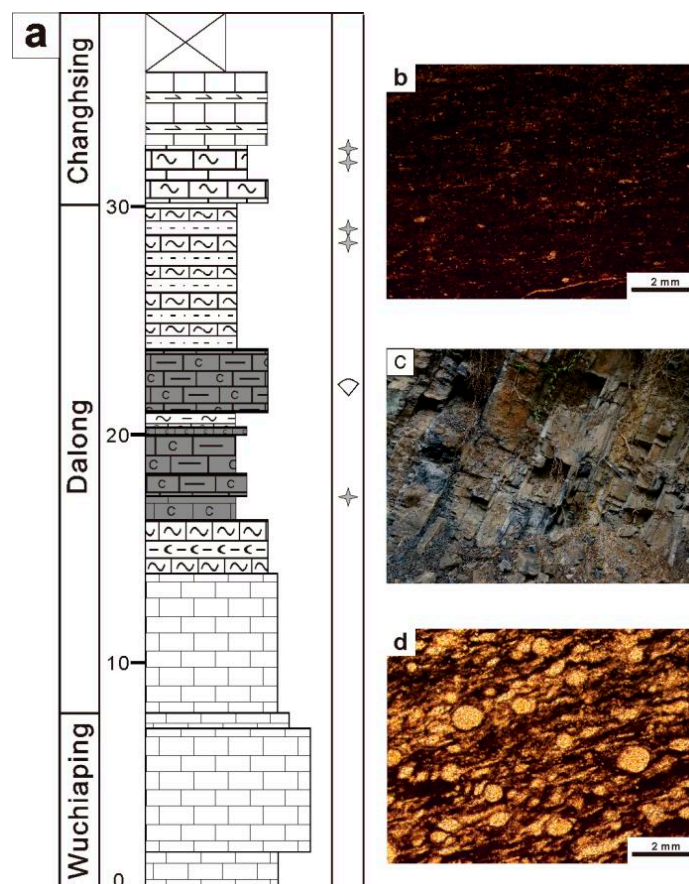


**Figure 3.** (a) Lithological column of the Jianfeng section. (b) Photomicrographs under plane-polarized light show carbonaceous limestone in the middle part of the Dalong Formation. (c) Volcanic ash in the middle Dalong Formation. (d) Photomicrographs under plane-polarized light show bedded chert bearing large numbers of radiolarians in the upper part of the Dalong Formation. See Figure 2 for legends.

### 3. Materials and Methods

Specimens were extracted from the Xibeixiang and Jianfeng stratigraphic sections, with meticulous attention paid to eliminating any weathered exteriors, as well as any post-depositional veins or voids, and discernible nodules or streaks. These specimens underwent fragmentation using a hammer, followed by a refinement process that employed the Rocklabs BTRM device to achieve a powdery consistency with a granularity of below 200 mesh. The resulting homogenized powders were then collected for the analyses.

For the determination of major elements, the lost-on-ignition (LOI) value was derived from the weight loss of the samples after they were subjected to combustion, a figure that was later utilized to adjust the measurements of elemental concentrations. Each sample

was weighed to a precision of 50 milligrams and then dissolved in an alkaline solution. The solution was acidified with nitric acid before being analyzed using an inductively coupled plasma optical emission spectrometer (ICP-OES) at the China University of Geosciences in Beijing. The precision of these analytical results was assured by comparing them against standard reference materials AGV-2, GSR-1, and GSR-5, with an accuracy of over 3%.

For the analysis of trace elements, approximately 100 milligrams of the finely ground samples were subjected to drying at a temperature of 980 °C for a duration of one hour. Subsequently, 40 milligrams of each sample were immersed in a mixture consisting of 1.5 mL of concentrated HNO<sub>3</sub> and 1.5 mL of HF, followed by heating at a temperature of 195 °C for 48 h within sealed Teflon containers. An additional 1 milliliter of HNO<sub>3</sub> was added to each sample, which was then evaporated almost to dryness. The samples were subsequently reconstituted with 2 mL of HNO<sub>3</sub> and 2 mL of Milli-Q water, and heated at 165 °C for 24 h to ensure thorough digestion. The samples were then diluted by a factor of 4000 and analyzed using an inductively coupled plasma-mass spectrometer (ICP-MS) at the China University of Geosciences. The precision of these analytical measurements was commonly greater than 5%, as monitored by the standards AGV-2, BHVO-2, W-2, GSR-1, and GSR-3, with the exception of phosphorus and potassium, which had a precision of less than 15%, and chromium, scandium, copper, zinc, strontium, and tantalum with a precision of less than 10%.

To determine the contribution from terrestrial sources and the authigenic components, the calculation of the trace element excess, denoted as  $X_{XS}$ , is essential. This is achieved using the equation:  $X_{XS} = X_{\text{sample}} - Al_{\text{sample}} \times (X/Al)_{\text{PAAS}}$ , where  $X_{\text{sample}}$  represents the concentration of the element X in the sample, and  $Al_{\text{sample}}$  denotes the aluminum concentration within the same sample. The term  $(X/Al)_{\text{PAAS}}$  refers to the ratio of element X to aluminum in the Post-Archean Australian shale, which serves as a benchmark [13]. In instances where the authigenic components may have been compromised, leading to negative  $X_{XS}$  values for some samples in this study, a standardization approach has been implemented. These negative values are adjusted to a uniform value of 0.01 ppm to facilitate the creation of log10 plots that depict the relationship between the trace element excess and depth. This adjustment ensures that the graphical representation remains informative and consistent.

## 4. Results

The geochemical data from Xibeixiang and Jianfeng sections are provided in the Supporting Information (Tables S1–S8).

The silicon content in the Dalong Formation at the Xibeixiang section varies significantly. The SiO<sub>2</sub> content ranges from 5.82% to 90.56%, with an average of 57.48%. The Fe/Ti ratios span from 1.49 to 225.39, averaging 24.92. Al/(Al + Fe + Mn) varies from 0.08 to 0.87, with an average of 0.57. In terms of trace elements, scandium (Sc) content ranges from  $0.45 \times 10^{-6}$  to  $10.04 \times 10^{-6}$ , averaging at  $3.23 \times 10^{-6}$ . Thorium (Th) content ranges from  $0.14 \times 10^{-6}$  to  $5.77 \times 10^{-6}$ , averaging at  $1.85 \times 10^{-6}$ . Lanthanum (La) content ranges from  $0.69 \times 10^{-6}$  to  $42.56 \times 10^{-6}$ , averaging at  $11.28 \times 10^{-6}$ . The Ti/Zr ratios vary from 5.18 to 36.16, with an average of 17.63, while the La/Sc ratios range from 0.91 to 27.19, averaging 3.92. The europium anomaly (Eu/Eu\*) values extend from 0.34 to 1.01, with a mean of 0.79. Standardized lutetium to lanthanum ratios (Lu<sub>N</sub>/La<sub>N</sub>) range from 0.63 to 2.77, with an average of 1.51.

In the Jianfeng section, the SiO<sub>2</sub> content varies from 5.05% to 93.64% (average value 56.27%). The Fe/Ti ratios span from 3.38 to 32.29, averaging 13.40%. Al/(Al + Fe + Mn) ratios vary from 0.34 to 0.85, with an average of 0.62. Regarding trace elements, Sc content ranges from  $0.48 \times 10^{-6}$  to  $22.58 \times 10^{-6}$ , averaging at  $6.17 \times 10^{-6}$ . The contents of Th

range from  $0.18 \times 10^{-6}$  to  $47.50 \times 10^{-6}$ , averaging at  $4.83 \times 10^{-6}$ . La content ranges from  $2.35 \times 10^{-6}$  to  $165.02 \times 10^{-6}$ , averaging at  $20.60 \times 10^{-6}$ . The Ti/Zr ratios range from 1.51 to 38.71, with an average of 18.70, while the La/Sc ratios range from 1.01 to 23.87, averaging at 4.40. The Eu/Eu\* values extend from 0.24 to 1.23, with an average of 0.90. Lastly, standardized  $\text{Lu}_N/\text{La}_N$  ranges from 0.63 to 2.01, averaging at 1.30.

## 5. Discussion

### 5.1. Origin of Siliceous Rocks

Aluminum (Al) and Titanium (Ti) co-occur in aluminosilicate minerals, serving as reliable indicators of terrestrial input. Conversely, iron (Fe) enrichment in sediments from mid-ocean ridges signifies hydrothermal activities [14]. Utilizing the Al-Fe-Mn triangular chart developed by Adachi et al. [15], which differentiates hydrothermal from non-hydrothermal siliceous rocks based on analyses of modern marine systems, the role of hydrothermal activities in sediment deposition can be assessed. The Al/(Al + Fe + Mn) ratio of marine sediments has also been used to measure the contribution of hydrothermal activities to sediment deposition [14]. It is reported that in the East Pacific Ridge hydrothermal system, this ratio can be as low as 0.01, indicating strong hydrothermal influence, while semi-oceanic siliceous sediments typically show a ratio of 0.60 [16]. The stronger the influence of hydrothermal activities is, the lower the Al/(Al + Fe + Mn) ratio becomes [15]. Similarly, Fe/Ti ratios could rise when sediment undergoes hydrothermal activities.

The Al-Fe-Mn triangle diagrams of the siliceous rocks of the Dalong Formation reveal that chert and siliceous limestone in Xibeixiang section are primarily of non-hydrothermal origin, while carbonate rocks in Xibeixiang section exhibit both hydrothermal and non-hydrothermal origins (Figure 4a). Furthermore, the chert and siliceous limestone in the Jianfeng section are solely of a non-hydrothermal origin, and the carbonate rocks also have no connection with hydrothermal activities (Figure 4b). These conclusions are consistent with the sedimentological characteristics, which show that the bedded chert and siliceous limestone of the Dalong Formation in the Xibeixiang and Jianfeng sections are rich in siliceous radiolarians, indicating that cherts and siliceous limestones have a biogenic origin rather than hydrothermal origin and are therefore biogenic. The mudstone and marly limestone in the Xibeixiang section contain multiple layers of volcanic ashes, which may be partly related to hydrothermal activities.

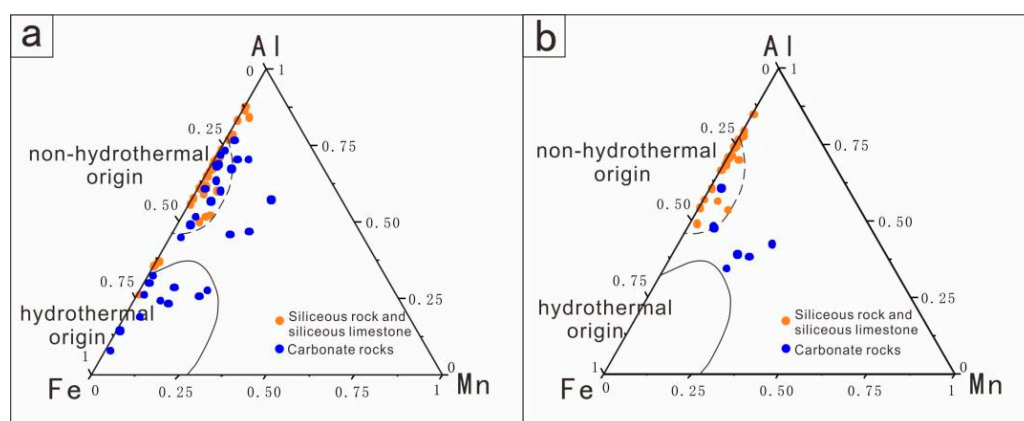


**Figure 4.** Al-Fe-Mn diagram of the Dalong Formation in the (a) Xibeixiang and (b) Jianfeng sections (after reference [15]).

The Al/(Al + Fe + Mn) ratios of the siliceous rocks in the Dalong Formation of the Xibeixiang section are predominantly above 0.6, and only a portion of the samples fall below 0.6, appearing in the marly limestone in the middle part of the Dalong Formation

(Figure 5). It suggests the minimal hydrothermal influence in the siliceous rocks in the Xibeixiang section and possible hydrothermal influence in the marly limestone. Similarly, in the Jianfeng section, siliceous rocks and siliceous limestone of the Dalong Formation consistently show  $Al/(Al + Fe + Mn)$  ratios greater than 0.6, while micrite, marly limestone, and bioclastic limestone exhibit ratios around 0.6.  $Fe/Ti$  ratios in both sections follow a similar pattern, particularly lower in the silicon-rich intervals. These findings align with the Al-Fe-Mn triangle diagram results, confirming that the source of silicon in the silicon-rich layers of the Dalong Formation in the Sichuan Basin is primarily biogenic rather than hydrothermal.

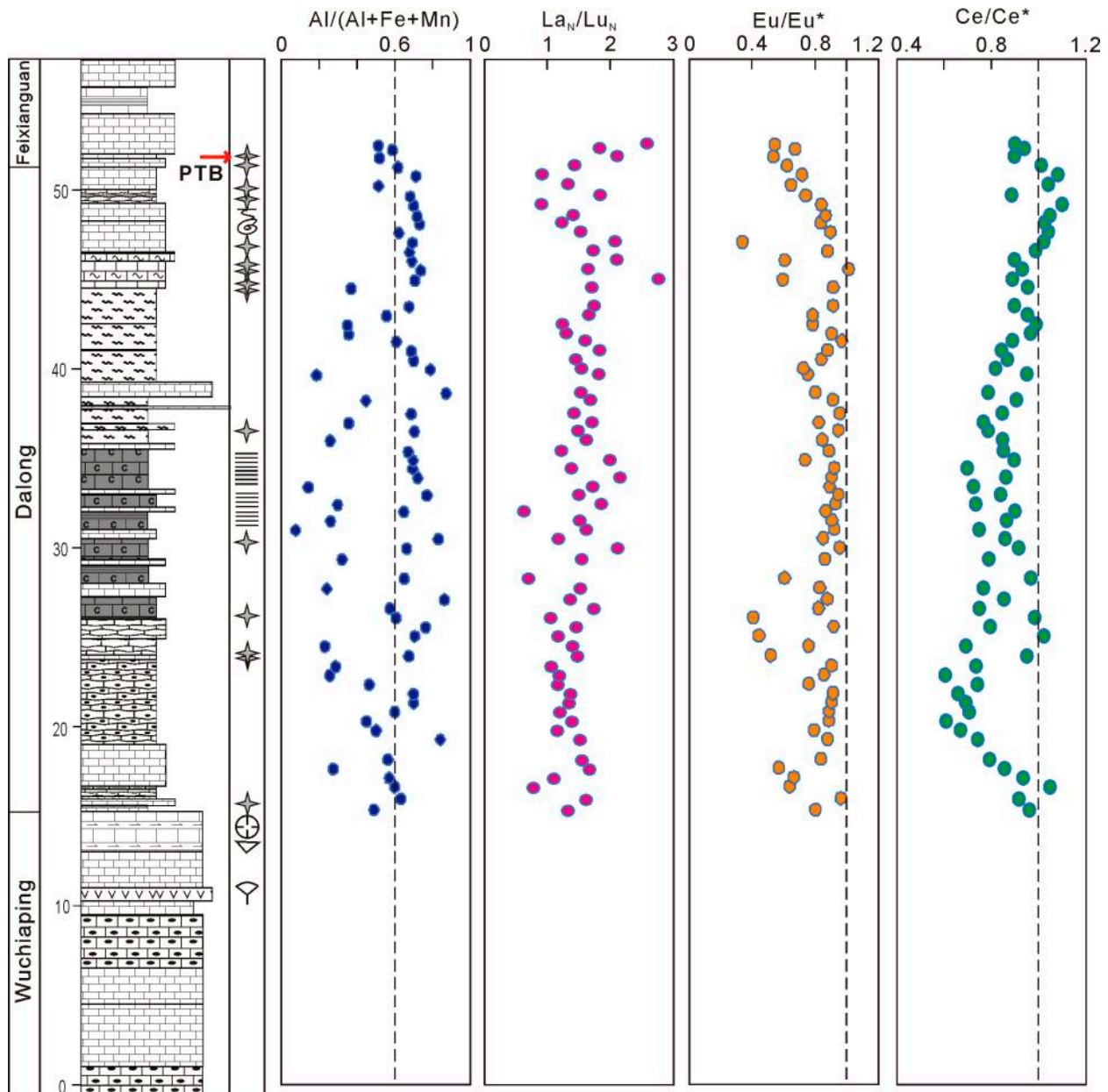


**Figure 5.** Chemostratigraphic profiles for the hydrothermal proxies of Dalong Formation in the Xibeixiang section. See Figure 2 for legends. The dotted line represents the boundary of the condition, as explained in detail in the text.

The anomaly of the rare earth element Europium (Eu) can indicate hydrothermal activity characteristics. In seawater, where rare earth elements predominantly exist as trivalent ions, Eu is unique as it presents in a divalent state ( $Eu^{2+}$ ) [17]. This special

valence state can lead to abnormal Eu eigenvalues. During magmatic activities,  $\text{Eu}^{3+}$  is often reduced to  $\text{Eu}^{2+}$ , which has a larger ionic radius than its neighboring rare earth elements, causing fractionation [18]. This reduction commonly occurs in the hydrothermal systems of mid-ocean ridges.  $\text{Eu}^{3+}$  can be reduced to  $\text{Eu}^{2+}$  in severely anoxic environments, and its ionic radius, similar to that of  $\text{Ba}^{2+}$ , facilitates its adsorption by barite, leading to precipitation [19]. The Eu fractionation often occurs in the hydrothermal system and leads to a positive anomaly of Eu [17], because the reduced  $\text{Eu}^{2+}$  is mainly absorbed by feldspar or other minerals due to the affinity of crystallization [20], resulting in Eu enrichment. The most pronounced Eu-positive anomalies are observed in seawater above hydrothermal fluids along mid-ocean ridges, with  $\text{Eu}/\text{Eu}^*$  values reaching up to 10 [20]. The  $\text{Eu}/\text{Eu}^*$  ratio in siliceous rocks typically decreases from 1.35 to 1.02 as the distance from the mid-ocean ridge increases, with Eu positive anomaly signals nearly disappearing 25 km (or 100 km) away from hydrothermal vents, although regional seawater may still be influenced by hydrothermal activities [21].

In the Dalong Formation at the Xibeixiang section, most  $\text{Eu}/\text{Eu}^*$  values are below 1.0 (Figure 5), suggesting a predominantly non-hydrothermal origin for the deposits. It is worth noting that  $\text{Eu}/\text{Eu}^*$  shows relatively high ratios in the marly limestone of the middle Dalong Formation, demonstrating the same conclusion as before. Furthermore,  $\text{Eu}/\text{Eu}^*$  ratios decline near the P-T boundary, probably due to the severe anoxia event in the P-T transition. Similarly, the Dalong Formation at the Jianfeng section shows mostly  $\text{Eu}/\text{Eu}^*$  values below 1.0, except for one instance in the marly limestone of the middle Dalong Formation, which exceeds 1.0, suggesting that the cherts of the Dalong Formation in the Jianfeng section are dominated by a non-hydrothermal origin. It is illustrated that the Sichuan Basin might have been close to the hydrothermal vent and affected by hydrothermal fluid to some extent during the deposition of the marly limestone.

In normal seawater, heavy rare earth elements (HREEs) exhibit more stable fluid chemical behavior due to their stronger inorganic complexation compared to light rare earth elements (LREEs) [22,23]. As a result, LREEs are more readily removed from seawater, leading to a seawater distribution pattern characterized by LREE deficiency [17]. Conversely, ocean basin hydrothermal fluids are enriched in LREEs [20], with significant absorption of LREEs from seawater by the hydrothermal fluids of mid-ocean ridges, leading to LREE depletion in surrounding seawater. Siliceous rocks, which primarily adsorb rare earth elements from seawater influenced by hydrothermal fluids, display a distribution pattern indicative of LREE depletion in mid-ocean ridge environments, with  $\text{Lu}_N/\text{La}_N$  ratios as high as 3 [24,25]. This ratio typically decreases with distance from the ridge, from 1.55 to 0.87, and further to 0.37 in normal ocean basins [21]. In open continental marginal seas, where LREEs are also removed from seawater, sediment  $\text{Lu}_N/\text{La}_N$  ratios reach around 1.10 [21].

In the cherts of the Dalong Formation at the Xibeixiang section, the  $\text{Lu}_N/\text{La}_N$  ratios are less than 3 and average at 1.51, suggesting that the Xibeixiang section was weakly influenced by hydrothermal fluids. It is noted that these ratios experience a dramatic increase to approximately 3 near the P-T boundary (Figure 5), which is confirmed by the decrease in  $\text{Al}/(\text{Al} + \text{Fe} + \text{Mn})$  ratios. Similarly,  $\text{Lu}_N/\text{La}_N$  peaked in the siliceous limestone of the upper Dalong Formation (Figure 5), which is also supported by the relatively low  $\text{Al}/(\text{Al} + \text{Fe} + \text{Mn})$  values and high  $\text{Eu}/\text{Eu}^*$  values exceeding 1. Combined with the volcanic ash interlayers, it is illustrated that the volcanic or hydrothermal activities only existed at the end-Permian. Moreover, most rare earth element distribution curves of the Xibeixiang section do not show LREE deficiency, with only a few samples exhibiting mild LREE depletion (Figure 6), suggesting that most of the deposition of Dalong formation was unrelated to hydrothermal events. As for the cherts of the Dalong Formation at the Jianfeng



section, the average of  $Lu_N/La_N$  ratios (1.30) is less than that at the Xibeixiang section (Figure 7), with no significant loss of LREEs observed (Figure 6). These findings suggest that the siliceous rocks in both the Xibeixiang and Jianfeng sections are predominantly of a non-hydrothermal origin. However, hydrothermal influences might have affected the Xibeixiang section near the P-T transition due to its proximity to the Paleo-Tethys.

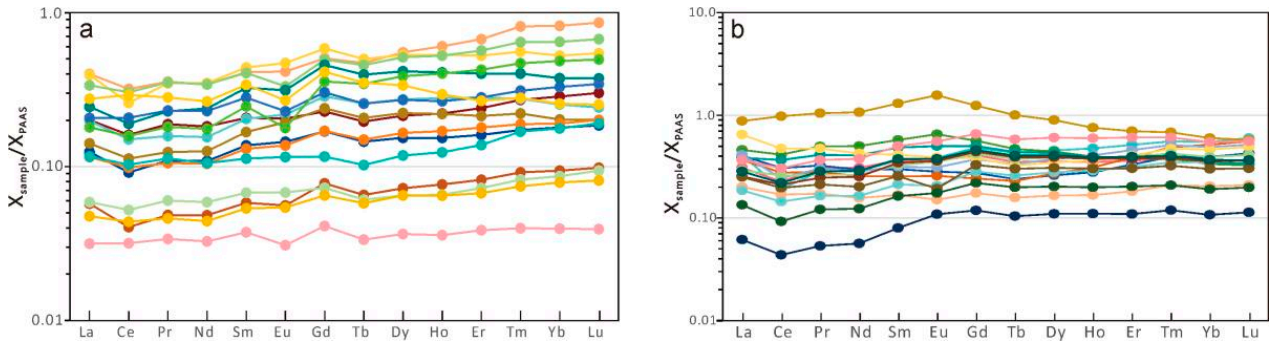


**Figure 6.** Post-Archean Australian shale (PAAS)-normalized REE pattern of the siliceous rock in the Dalong Formation at (a) the Xibeixiang section and (b) the Jianfeng section.

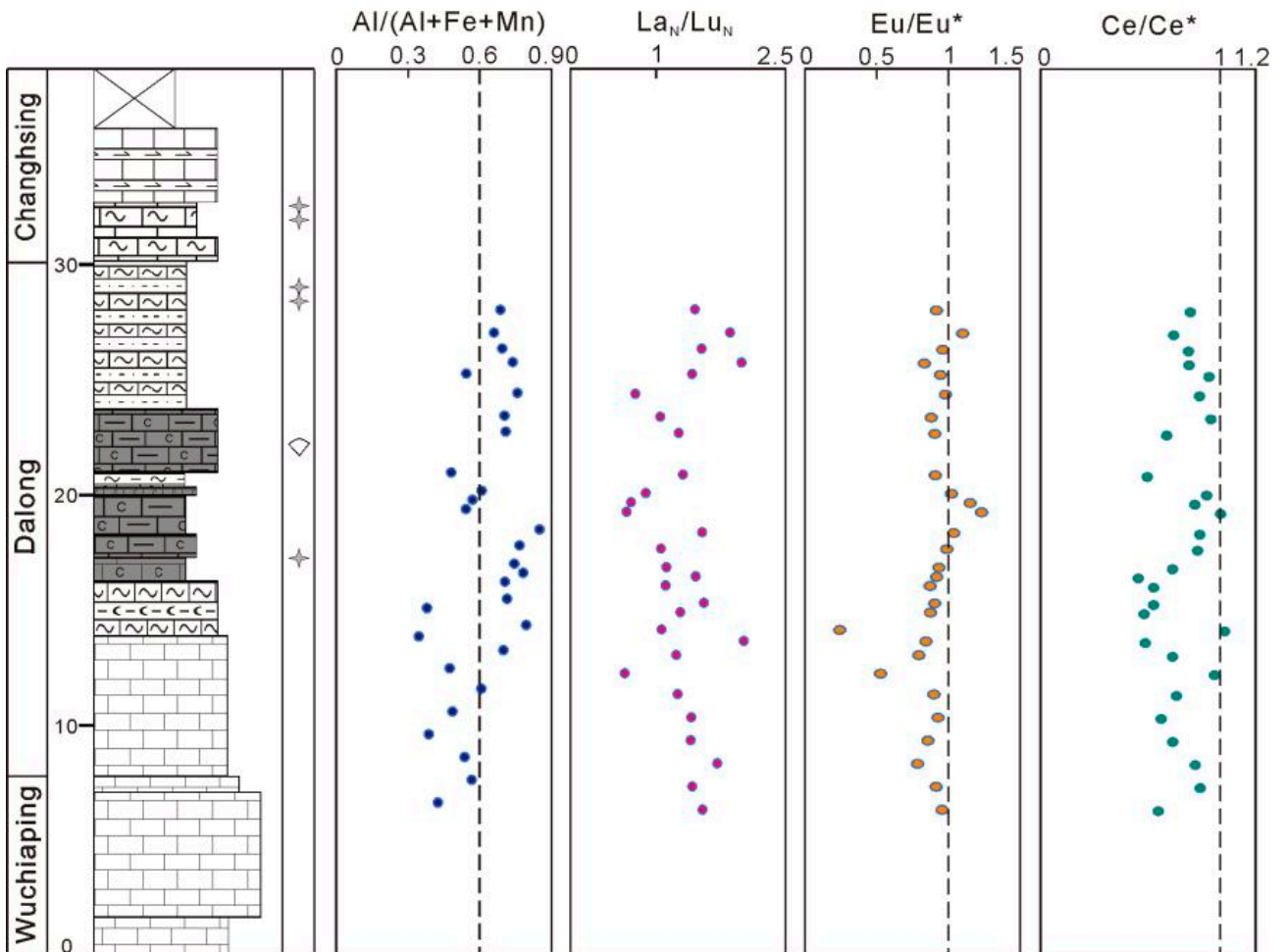


**Figure 7.** Chemostratigraphic profiles for the hydrothermal proxies of the Dalong Formation in the Jianfeng section. See Figure 2 for legends.

Cerium (Ce) typically exists as  $Ce^{3+}$  in marine environments, which can be easily oxidized to the less soluble  $Ce^{4+}$  and precipitate under oxidative conditions. Therefore, positive Ce anomalies or  $Ce/Ce^*$  ratios close to 1 in marine sediments often indicate anoxic

conditions [13]. In both the Xibeixiang and Jianfeng sections, the  $Ce/Ce^*$  values exhibit an upward trend from the bottom to the top of the Dalong Formation, approaching 1 in the middle and upper parts. Combined with former studies [26], it is reported that the depositional environment of the upper and middle Dalong Formation was anoxic, and the organic accumulation was primarily driven by productivity. Data on rare earth element contents and ratios further suggest that the formation of this anoxic environment and the associated enrichment of organic matter were largely independent of hydrothermal activities.

### 5.2. Sedimentary Tectonic Background of the Dalong Formation

Certain inert trace elements such as La, Zr, Ce, Nd, Y, Hf, Nb, Ti, Sc, and Th are key indicators of the tectonic background and provenance of sedimentary deposits due to their minimal migration during sedimentation and short residence times in seawater [27]. These elements are consistently delivered to clastic sedimentary rocks through weathering and transportation, thereby offering distinct indicators that can be traced back to their original rock formations [27]. The La-Th-Sc triangulation chart effectively differentiates various tectonic settings. Oceanic island arc environments typically show higher Sc contents and lower La/Sc ratios (average  $0.55 \pm 0.2$ ), continental margins have higher La contents with La/Sc ratios around 4, and continental island arcs exhibit moderate La/Sc ratios (average  $0.8 \pm 0.3$ ) [28]. Although this chart can distinguish between Paleozoic oceanic and continental island arcs, it is difficult to distinguish between active and passive continental margins. However, the intersection chart of La/Sc and Ti/Zr ratios helps in this differentiation [29]. Samples from oceanic island arcs are identified by titanium-to-zirconium (Ti/Zr) ratios that exceed 40 and lanthanum-to-scandium (La/Sc) ratios that surpass 1. In contrast, continental island arcs display Ti/Zr ratios within the range of 10 to 35 and La/Sc ratios that fall between 1 and 3. Active continental margins are distinguished by elevated La/Sc ratios, which range from 3 to 6. Conversely, passive continental margins are indicated by Ti/Zr ratios that are below 10 and La/Sc ratios from 3 to 9 [29].

The siliceous rocks of the Dalong Formation in the Xibeixiang and Jianfeng sections do not display oceanic island arc characteristics. In the Xibeixiang section, the predominant tectonic settings are continental island arcs and active continental margins, with a minor component of passive continental margins (Figures 8a and 9a). On the other hand, the Jianfeng section indicates geologic characteristics of both a continental island arc and an active continental margin, devoid of the attributes typically associated with a passive continental margin, as illustrated in Figures 8b and 9b. Hydrothermal processes are known to be particularly pronounced in regions of active continental margins and oceanic island arcs. The absence of oceanic island arc traits in these sections suggests that the northeast Sichuan basin was distant from major hydrothermal activities. Nonetheless, the proximity of the Xibeixiang section to the Paleo-Tethys may explain its more pronounced hydrothermal signals compared to the Jianfeng section.

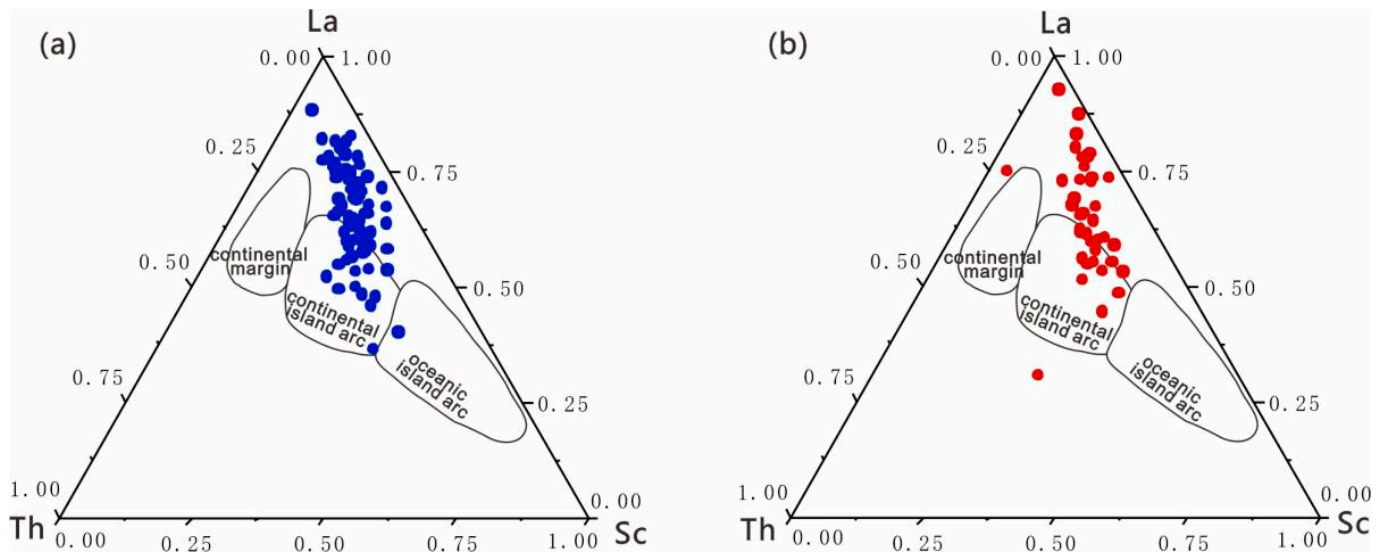


**Figure 8.** La-Th-Sc diagram of Dalong cherts at (a) the Xibeixiang section and (b) the Jianfeng section (base map after reference [29]).

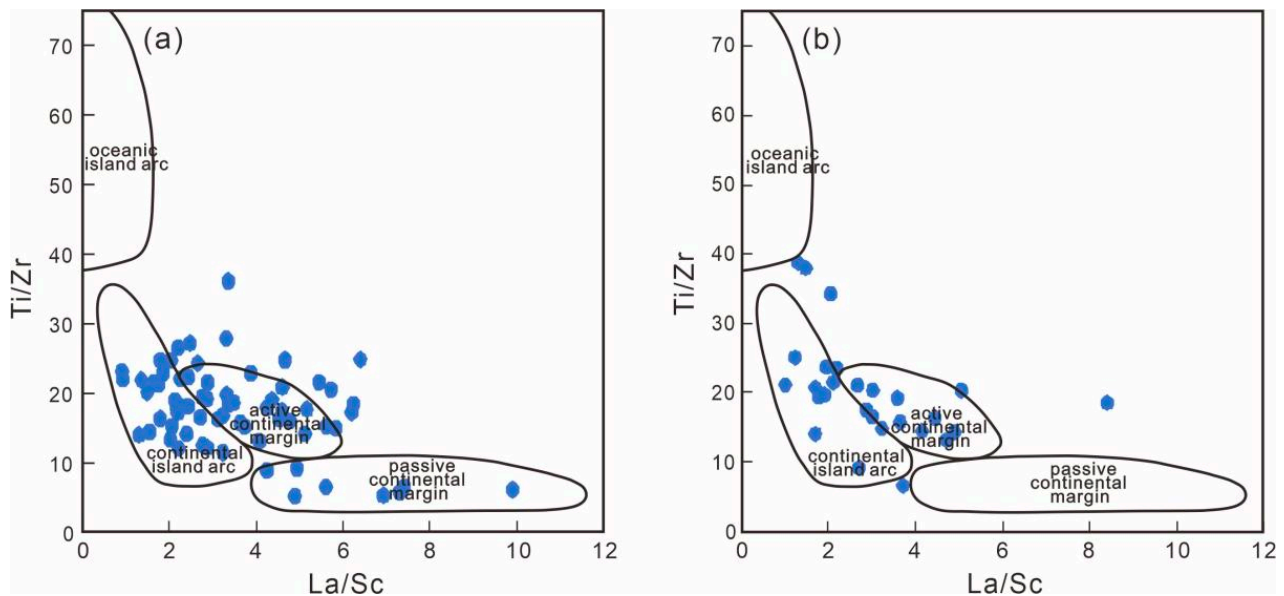


**Figure 9.** Cross-plot between La/Sc and Ti/Zr of Dalong cherts at (a) the Xibeixiang section and (b) the Jianfeng section (base map after reference [29]).

### 5.3. Influence of Hydrothermal Activity on Organic Matter Enrichment

As discussed above, the siliceous rocks in the upper part of the Dalong Formation are more likely to have non-hydrothermal origins. A large number of radiolarians observed in photomicrographs demonstrated that the source of siliceous rocks in both the Xibeixiang and Jianfeng sections leans more toward biological origins. The carbonate rocks of the middle Dalong Formation and P-T boundary in the Xibeixiang section show more hydrothermal characteristics. Previous studies, however, suggested that the organic enrichment and high primary productivity emerged in parallel with the ampelitic limestone, and the anoxic environment appeared during the deposition of marly limestone and chert. The weak correlation between TOC and indicators of hydrothermal activities (Figure 10) indicates that the organic accumulation is less likely to be related to the hydrothermal activities.

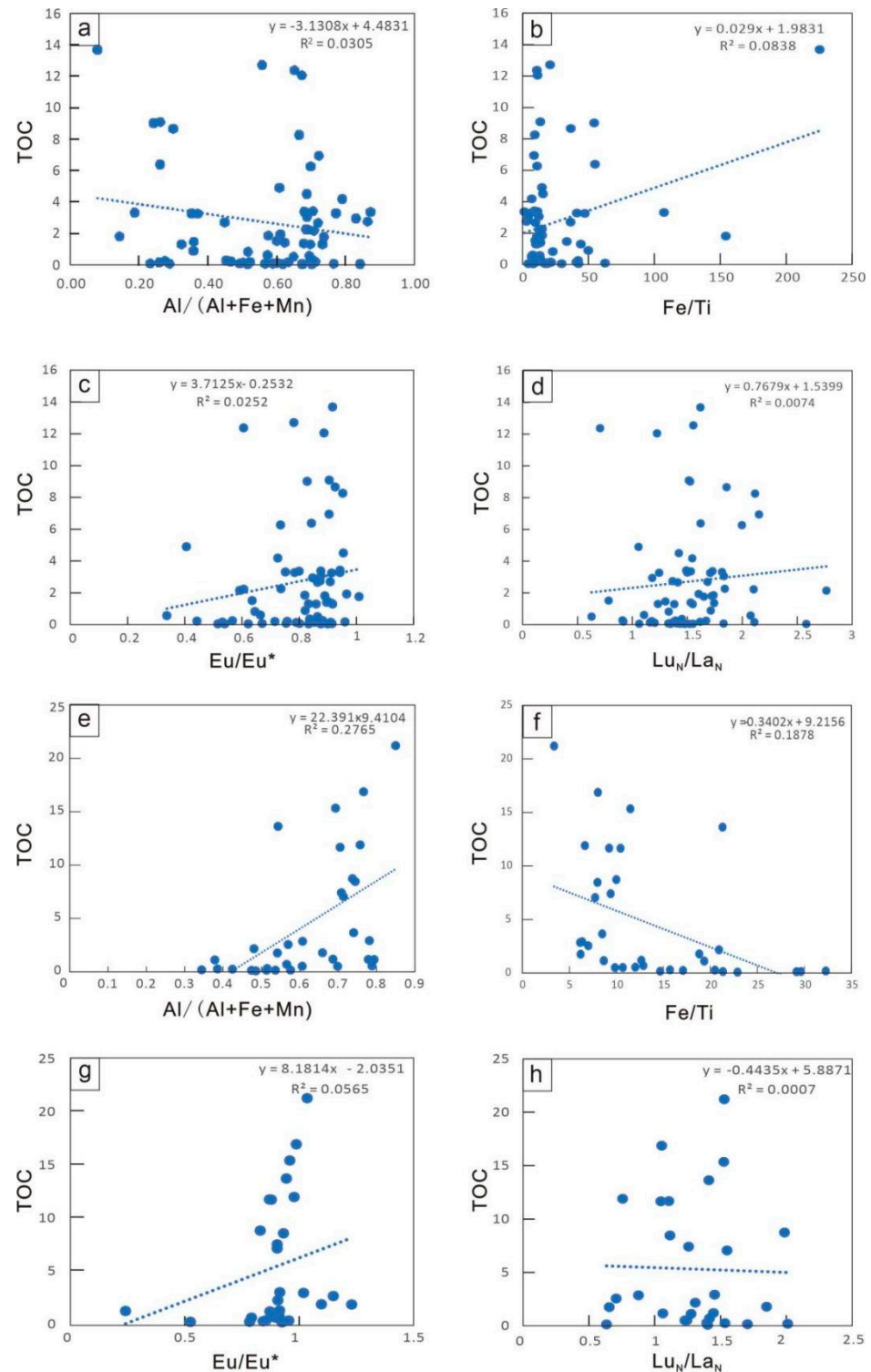


**Figure 10.** Cross-plot between TOC and indicators of hydrothermal activities in (a–d) the Xibeixiang section and (e–h) the Jianfeng section.

## 6. Conclusions

The silicon source of the cherts and siliceous limestone of the Dalong Formation at the Xibeixiang and Jianfeng sections is predominantly biogenic, as evidenced by the abundance of radiolarians, and shows minimal influence from hydrothermal activities, as documented by the rare earth element proxies. However, the mudstone and marly limestone in the Xibeixiang section could be affected by hydrothermal activities, as suggested by the  $Eu/Eu^*$  ratios and the presence of several volcanic ash layers observed in the field. Furthermore, the

middle part of the marly limestone in the Jianfeng section may retain a weaker hydrothermal signal compared to the Xibeixiang section. The tectono-sedimentary background of the Dalong Formation in the Xibeixiang section primarily consists of continental island arcs and active continental margins, with a minor component of passive continental margins. Conversely, the cherts and siliceous limestone in the Jianfeng section reflect a continental island arc and active continental margin setting. The lack of oceanic island arc characteristics in both sections indicates that the northeast Sichuan basin is distant from significant hydrothermal activity zones. Notably, the active continental margin features of the siliceous rocks in the Xibeixiang section are more marked than those in the Jianfeng section, likely due to its proximity to the open marine environments during the Late Permian, which might have allowed it to retain subtle signs of hydrothermal activities. The weak correlation between TOC and indicators of hydrothermal activities demonstrates that hydrothermal activity had minimal impact on the formation of anoxic environments and the enrichment of organic matter during the deposition of the Dalong Formation.

**Supplementary Materials:** The following supporting information can be downloaded at: <https://www.mdpi.com/article/10.3390/min15010069/s1>, Table S1: XBX major elements; Table S2: XBX Eu anomaly; Table S3: XBX Ce anomaly; Table S4: XBX rare elements; Table S5: JF major elements; Table S6: JF Eu anomaly; Table S7: JF Ce anomaly; Table S8: JF rare elements;

**Author Contributions:** Conceptualization, R.W.; methodology, X.G. (Xiaotong Ge); formal analysis, X.G. (Xiaotong Ge) and X.G. (Xun Ge); investigation, X.G. (Xun Ge); data curation, X.G. (Xiaotong Ge); writing—original draft preparation, X.G. (Xiaotong Ge) and M.L.; writing—review and editing, D.C.; supervision, D.C. and Y.L.; funding acquisition, D.C. and Y.L. All authors have read and agreed to the published version of the manuscript.

**Funding:** This study was supported by the National Natural Science Foundation of China (91755210) and the Science and Technology Project of SINOPEC (P24207).

**Data Availability Statement:** The data presented in this study are available in Supplementary Materials.

**Acknowledgments:** The researchers extend their gratitude to Hongyu Zhang and Zihu Zhang for their contributions to the laboratory work. The valuable feedback and recommendations provided by the editorial team and peer reviewers are also greatly appreciated.

**Conflicts of Interest:** The authors declare that this study received funding from the National Natural Science Foundation of China (91755210) and the Science and Technology Project of SINOPEC (P24207). The funder had the following involvement with the study: supervision, funding acquisition and writing—review and editing.

## References

1. Cao, T.T.; Song, Z.G.; Wang, S.B.; Cao, X.; Li, Y.; Xia, J. Characterizing the pore structure in the Silurian and Permian shales of the Sichuan Basin, China. *Mar. Pet. Geol.* **2015**, *61*, 140–150. [[CrossRef](#)]
2. Wei, Z.F.; Wang, Y.L.; Wang, G.; Sun, Z.; Xu, L. Pore characterization of organic-rich Late Permian Da-long Formation shale in the Sichuan Basin, southwestern China. *Fuel* **2018**, *211*, 507–516. [[CrossRef](#)]
3. Wang, R.Y.; Hu, Z.Q.; Dong, L.; Gao, B.; Sun, C.; Yang, T.; Wang, G.; Yin, S. Advancement and trends of shale gas reservoir characterization and evaluation. *Oil Gas Geol.* **2021**, *42*, 54–65.
4. Fang, S.Y. Middle-Upper Permian Siliceous Rocks in Lower Yangtze Area Origin and Shale Gas Potential. Master's Thesis, Nanjing University, Nanjing, China, 2021.
5. Xu, Y.T. Genetic geochemistry for the bedded silicalite in the late permian Dalong formation and its sedimehtary setting in Southeastern Hubei. *J. Guilin Inst. Technol.* **1997**, *17*, 204–212. (In Chinese with English Abstract)
6. Li, F.; Liu, Z.J.; Chen, F.R.; Wei, F.B.; Guo, J.C.; Su, Z.X. Origin of siliceous mudstone in Permian Dalong Formation and its influence on compressibility, Northeastern Sichuan Basin. *Nat. Gas Geosci.* **2023**, *34*, 349–358. (In Chinese with English Abstract)
7. Fang, X.; Zhou, Y.Q.; Yao, X.; Liu, M.C.; Liu, J.Z. Geochemical characteristics and petrogenesis of siliceous rocks from Shansi section, Guangyuan, Sichuan Province. *Miner. Pet.* **2017**, *37*, 93–102. (In Chinese with English Abstract)

8. Yang, Y.C. Research on Geochemical Characteristics and Formative Factors of Cherts in the Dalong Formation of the Shangjianggou Area, Northwestern Sichuan Basin. Master's Thesis, Chengdu University of Technology, Chengdu, China, 2015.
9. Mei, S.; Henderson, C.M. Evolution of Permian conodont provincialism and its significance in global correlation and paleoclimate implication. *Palaeogeogr. Palaeoclimatol. Palaeoecol.* **2001**, *170*, 237–260. [[CrossRef](#)]
10. Wignall, P.B.; Hallam, A.; Lai, X.; Yang, F. Palaeoenvironmental changes across the Permian/Triassic boundary at Shangsi (N. Sichuan, China). *Hist. Biol.* **1995**, *10*, 175–189. [[CrossRef](#)]
11. Luo, J.X.; He, Y.B. Anoxic environments of the Permian of Middle and Upper Yangtze Area. *J. Palaeogeogr.* **2011**, *13*, 11–20. (In Chinese with English Abstract)
12. Shellnutt, J.G.; Denyszyn, S.W.; Mundil, R. Precise age determination of mafic and felsic intrusive rocks from the Permian Emeishan large igneous province (SW China). *Gondwana Res.* **2012**, *22*, 118–126. [[CrossRef](#)]
13. Tribouillard, N.; Algeo, T.J.; Lyons, T.; Riboulleau, A. Trace metals as paleoredox and paleoproductivity proxies: An update. *Chem. Geol.* **2006**, *232*, 12–32. [[CrossRef](#)]
14. Murray, R.W. Chemical criteria to identify the depositional environment of chert: General principles and applications. *Sediment. Geol.* **1994**, *90*, 213–232. [[CrossRef](#)]
15. Adachi, M.; Yamamoto, K.; Sugisaki, R. Hydrothermal chert and associated siliceous rocks from the northern Pacific: Their geological significance as indication of ocean ridge activity. *Sediment. Geol.* **1986**, *47*, 125–148. [[CrossRef](#)]
16. Boström, K.; Peterson, M.N.A. The origin of aluminum-poor ferromanganoan sediments in areas of high heat flow on the East Pacific Rise. *Mar. Geol.* **1969**, *7*, 427–447. [[CrossRef](#)]
17. De Baar, H.J.W.; Bacon, M.P.; Brewer, P.G.; Bruland, K.W. Rare earth elements in the Pacific and Atlantic Oceans. *Geochim. Cosmochim. Acta* **1985**, *49*, 1943–1959. [[CrossRef](#)]
18. Michard, A.; Albarède, F.; Michard, G.; Minster, J.F.; Charlou, J.L.; Albar, F. Rare-earth elements and uranium in high-temperature solutions from East Pacific Rise hydrothermal vent field (13° N). *Nature* **1983**, *303*, 795–797. [[CrossRef](#)]
19. Kimata, M. The crystal structure of non-stoichiometric Eu-anorthite: An explanation of the Eu-positive anomaly. *Mineral. Mag.* **1988**, *52*, 257–265. [[CrossRef](#)]
20. Michard, A. Rare earth element systematics in hydrothermal fluids. *Geochim. Cosmochim. Acta* **1989**, *53*, 745–750. [[CrossRef](#)]
21. Murray, R.W.; Buchholtz Ten Brink, M.R.; Gerlach, D.C.; Russ, G.P., III; Jones, D.L. Rare earth, major, and trace elements in chert from the Franciscan Complex and Monterey Group, California: Assessing REE sources to fine-grained marine sediments. *Geochim. Cosmochim. Acta* **1991**, *55*, 1875–1895. [[CrossRef](#)]
22. Goldberg, E.D.; Koide, M.; Schmitt, R.A.; Smith, R.H. Rare-earth distributions in the marine environment. *J. Geophys. Res.* **1963**, *68*, 4209–4217. [[CrossRef](#)]
23. Turner, D.R.; Whitfield, M.; Dickson, A.G. The equilibrium speciation of dissolved components in freshwater and sea water at 25 °C and 1 atm pressure. *Geochim. Cosmochim. Acta* **1981**, *45*, 855–881. [[CrossRef](#)]
24. Baker, R.A. Trace inorganics in water. In *Neutron Activation Analysis of Lanthanide Elements in Sea Water*; Høgdahl, O.T., Melsom, S., Bowen, V.T., Eds.; Jenne E A: Washington, DC, USA, 1968; pp. 308–325.
25. Klinkhammer, G.; Elderfield, H.; Hudson, A. Rare earth elements in seawater near hydrothermal vents. *Nature* **1983**, *305*, 185–188. [[CrossRef](#)]
26. Ge, X.T.; Chen, D.Z.; Zhang, G.J.; Huang, T.; Liu, M.; El-Shafeiy, M. Marine redox evolution and organic accumulation in an intrashelf Basin, NE Sichuan Basin during the Late Permian. *Mar. Pet. Geol.* **2022**, *140*, 105633. [[CrossRef](#)]
27. Holland, H.D. *The Chemistry of the Atmosphere and Oceans*; Wiley: New York, NY, USA, 1978.
28. McLennan, S.M.; Taylor, S.R.; Kröner, A. Geochemical evolution of Archean shales from South Africa. I. The Swaziland and Pongola Supergroups. *Precambrian Res.* **1983**, *22*, 93–124. [[CrossRef](#)]
29. Bhatia, M.R.; Crook, K.A.W. Trace element characteristics of graywackes and tectonic setting discrimination of sedimentary basins. *Contrib. Mineral. Petrol.* **1986**, *92*, 181–193. [[CrossRef](#)]

**Disclaimer/Publisher's Note:** The statements, opinions and data contained in all publications are solely those of the individual author(s) and contributor(s) and not of MDPI and/or the editor(s). MDPI and/or the editor(s) disclaim responsibility for any injury to people or property resulting from any ideas, methods, instructions or products referred to in the content.